In Vivo Bioluminescence Imaging Study to Monitor Ectopic Bone Formation by Luciferase Gene Marked Mesenchymal Stem Cells

Cristina Olivo,[1] Jacqueline Alblas,[2] Vivienne Verweij,[1] Anton-Jan Van Zonneveld,[3] Wouter J.A. Dhert,[2] Anton C.M. Martens[1]

[1]Department of Immunology, UMC Utrecht, HP: KC02.085.2, Lundlaan 6, 3584 EA Utrecht, The Netherlands, [2]Department of Orthopaedics, UMC Utrecht, Utrecht, The Netherlands, [3]Department of Nephrology, Leiden University Medical Center, Leiden, the Netherlands

ABSTRACT: Mesenchymal stem cells (MSCs) represent a powerful tool for applications in regenerative medicine. In this study, we used in vivo bioluminescence imaging to noninvasively investigate the fate and the contribution to bone formation of adult MSCs in tissue engineered constructs. Goat MSCs expressing GFP-luciferase were seeded on ceramic scaffolds and implanted subcutaneously in immune-deficient mice. The constructs were monitored weekly with bioluminescence imaging and were retrieved after 7 weeks to quantify bone formation by histomorphometry. With increasing amounts of seeded MSCs (from 0 to 1×10^6 MSC/scaffold), a cell-dose related increase in bioluminescence was observed at all time points, correlating with increased bone formation at 7 weeks. To investigate the relevance of MSC proliferation to bone deposition, cell-seeded scaffolds were irradiated. The irradiated cells were functional with respect to oxygen consumption but no increase in bioluminescence was observed in vivo, and only minimal bone was produced. Proliferating MSCs are likely required for initiation of bone formation in tissue engineered constructs in vivo. Bioluminescence is a useful tool to monitor cellular responses and predict bone formation in vivo. © 2008 Orthopaedic Research Society. Published by Wiley Periodicals, Inc. J Orthop Res

Keywords: tissue engineering; luciferase; stem cell research; osteogenesis; bioluminescence imaging

The presence of a bone defect often requires interventions to augment normal healing. Mesenchymal stem cells (MSC)-seeded scaffolds are an alternative to autologous bone graft for enhancing bone healing. MSCs derived from adult bone marrow[1] differentiate in vitro to the osteoblast lineage to produce mineralized bone matrix. Bone formation results when MSCs are seeded on appropriate biomaterials such as biphasic calcium phosphate (BCP) in ectopic sites.[2–4]

Noninvasive strategies to monitor cells in vivo, such as bioluminescence imaging (BLI), have been applied for studies on bone regeneration in transgenic animals[5] or to visualize fibroblasts in ectopic implants[6] and MSCs in a spinal fusion model.[7] However, the behavior of MSCs is still not fully understood, though such information is fundamental for optimal application of stem cells to bone tissue engineering.[8] We used BLI of luciferase-gene marked MSCs after seeding increasing numbers on scaffolds followed by implantation subcutaneously in immune-deficient mice. Some scaffolds were gamma-irradiated prior to implantation to reduce the outgrowth of the seeded MSCs. MSC cultures have high radio-resistance and do not display substantial cell death[9] even after high doses. The surviving cell fraction shows a dose-dependent decrease in proliferative potential, together with reduced osteogenic potential,[10] while the capacity to produce growth factors is preserved.[11,12] We correlated the amount of cells seeded on the scaffolds, the increase in bioluminescence, and the amount of bone formed in vivo. To gain insight in the contribution of seeded cells in bone tissue engineering, hybrid scaffolds were irradiated prior to implantation, resulting in low luciferase activity and minimal amounts of bone.

METHODS

Cell Cultures

Bone marrow stem cells were isolated by density gradient centrifugation from iliac bone marrow aspirates of two adult goats. Cells were seeded at 4×10^5 cells/cm^2 in 45% RPMI culture medium, 45% Dulbecco's modified Eagle's medium (DMEM), streptomycin (0.1 mg/ml), penicillin (100 IU/ml; Gibco Life Technology, Pasley, Scotland), and 10% fetal calf serum (FCS) (Cambrex, Vervier, Belgium) and cultured in 5% CO$_2$ at 37°C. MSCs were selected by plastic adherence. At passage 3, colony forming units-culture (CFU-F) and colony forming units-osteoblasts (CFU-O) assays were performed according to the manufacturer's instructions (Stem Cell Technologies, Meylane, France).

Retroviral Vector and Transduction

To construct the LZRS-GFP-luciferase retroviral vector, encoding a fusion protein of green fluorescent protein (GFP) and luciferase, the IRES-EGFP sequence was removed from the LZRS-pBMN-IRES-EGFP vector (S-001-AB provided by Dr. G. Nolan) and replaced with GFP-luciferase (provided by Dr. R. Day[13]). Amphotrophic virus supernatant was produced using Phoenix cells (provided by Dr. G. Nolan). The viral titer of the supernatant determined on NIH-3T3 cells was 2.8×10^5 infectious virus particles/ml. Goat MSCs were seeded at 10^5 cells/cm^2 and incubated overnight with LZRS-GFP-luciferase amphotropic virus (undiluted) and polybrene (8 µg/ml; Sigma). After 48 h, the cell fraction expressing GFP was quantified by fluorescence activated cell sorting (FACS) analysis and luciferase activity was quantified by in vitro luciferase activity assay (Promega, Madison, WI, USA).

Mineralization Assay

MSCs (passage 4–6) were seeded in 6-well plates. Osteogenic differentiation was induced for 21 days by adding 10 mM β-glycerophosphate (Sigma), 10^{-8} M dexamethasone (Dex; Sigma-Aldrich Chemie GmbH, Schellendorf, Germany), and 50 µg/ml ascorbic acid to the medium. Mineralization was assessed by alizarin red (Sigma) staining and quantified by a spectrophotometer, after dissolution of the dye in 100 mM cetylpyridinumchloride (Sigma).

Scaffolds and Cell Seeding

To prepare hybrid implants, GFP-luciferase transduced MSCs were statically seeded on BCP scaffolds of $4 \times 4 \times 4$ mm (weight 250 mg). Scaffolds were made of 50%–60% macroporous BCP (OsSatura[TM], IsoTis, The Netherlands) consisting of $80\% \pm 5\%$ hydroxyapatite and $20\% \pm 5\%$ tricalcium phosphate. Interconnected macroporosity was created by H_2O_2 foaming resulting in 100–1,000 µm pores. The material was then sintered at $1,200°C$ resulting in $15\% \pm 5\%$ microporosity (1–10 µm).[14] Scaffolds were cleaned ultrasonically and steam sterilized. For the first experiment, six groups of scaffolds ($n = 3$) were seeded with 0, 0.05, 0.125, 0.25, 0.5, or 1×10^6 MSC/scaffold and implanted in three mice. For the second experiment, five groups of scaffolds were prepared ($n = 6$ per group) by seeding 0, 0.5, 1, 0.5 irradiated, or 1×10^6 irradiated cells/scaffold. A final two groups were prepared by irradiating seeded scaffolds with a dose of 20 Gray. For each mouse, five scaffolds (one per group) were implanted 20 h after seeding.

Cell Viability and In Vitro BLI

Prior to implantation, cell viability and presence of GFP-luciferase positive MSCs were asserted in an oxygen binding system assay (BD Bioscience, Erembodegem, Belgium) that quantifies the cellular consumption of oxygen. Subsequently, the presence of transduced MSCs on the scaffolds was quantified by BLI, by adding 50 mg/ml D-luciferin (Synchem Chemie, Kassel, Germany) dissolved in PBS (Gibco) to the scaffolds and imaging the bioluminescent signal for 5 min (see below). Scaffolds were then replaced in culture medium and implanted.

Animals

Animal experiments were conducted with permission from the Ethical Committee for Animal Experimentation and according to Institutional Guidelines on the use of animals. Immune-deficient RAG2-γc, double KO mice[15] were obtained from the Netherlands Cancer Institute (Amsterdam), bred and maintained in filter-top cages. They were given radiation-sterilized food pellets and distilled water ad libitum. After surgery, the analgesic temgesic (0.05 mg/kg body weight; Bayer Leverkasen, Germany) and antibiotic ciproxin (100 mg/ml; Bayer) were added to the water daily.

Surgery and Bioluminescence Imaging (BLI)

Mice were anesthetized with 0.2 µl/g body weight of ketamine, xylazine, and atropine solution (ratio of 1:1.25:0.75). To minimize interference of the bioluminescence signals from different samples, each scaffold was inserted in a separate subcutaneous pocket on the dorsal side. Before BLI measurement, animals were anesthetized with an intramuscular injection of the above solution, shaved, and injected intraperitoneally with D-luciferin dissolved in PBS (125 mg/kg body weight). BLI was performed as previously described,[5] using a Roper bioluminescence Imaging System Princeton Instruments, Trenton, NJ, USA. The cooled charge-coupled device camera (LN/CCD-1300EB) was equipped with a 50-mm F1.2 Nikon lens (Roper Scientific) and controlled by Metavue software (Universal Imaging Corp., West Chester, PA, USA). BLI images were acquired over 20 min. Exposure conditions (time, aperture, stage position, binning, and time after injection) were kept identical in all measurements. Bioluminescence intensity images were pseudo-colored (blue least intense and white most intense) and quantified using MetaMorph software (Universal Imaging Corp.). For quantification, a standard region of interest (ROI) was defined for all measurements. Within the ROI, background noise and bioluminescence intensity at signal saturation (between 15 and 20 min) were used to calculate the average intensity. Measurements were expressed as relative light units per minute (RLU).

Histology

At day 46, animals were euthanized with an overdose of the anesthesia solution. Scaffolds were retrieved, fixed with 4% paraformaldehyde, decalcified for 5 days in 12.5 % w/v EDTA in demineralized water, and embedded in paraffin; 10 µm sections were stained with H&E.[16] Osteoclasts were identified by TRAP staining. Areas stained positive were scored as 1 for a small, 2 for an intermediate, and 3 for a large area.

GFP-luciferase transduced cells were revealed by immunohistochemistry using the anti-GFP antibody (Ab 6556 from Abcam, Cambridge, UK). Sections were treated with 1.5% H_2O_2 and incubated with ab 6556 (1:2000 in PBS) overnight at 4°C, then with biotinylated swine anti-rabbit immunoglobulin G (IgG) (1:800 in PBS) for 2 h at room temperature. Finally, samples were incubated with avidin-biotinylated enzyme complex/horseradish peroxidase (ABC-complex/HRP) for 30 min and then detected using 3,3′-diaminobenzidine (DAB) staining. Counterstaining was performed with Mayer's hematoxylin. All secondary antibodies were from DAKO Cytomation Glostrup, Denmark.

Blood vessels were quantified by counting all erythrocyte-containing vessels per section. The results were averaged and expressed as number of vessels per scaffold.

Histomorphometry

Scaffolds were photographed at $4\times$ magnification, and an image of the scaffold rebuilt using Adobe Photoshop CS2. Three images per scaffold were reconstituted and analyzed by Zeiss-KS400 software, using a custom program. An area of
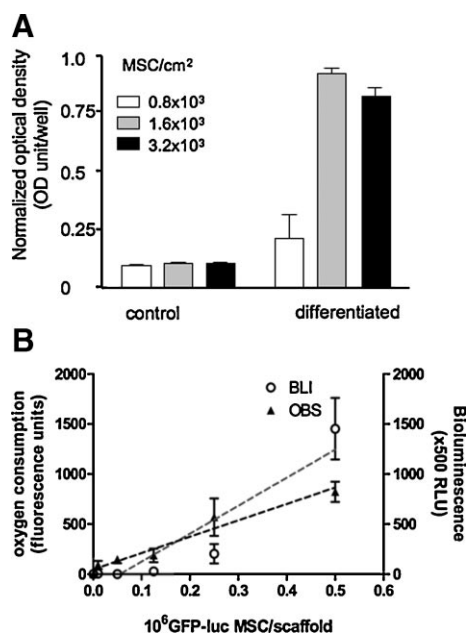

Figure 1. (A) MSCs seeded at different densities (0.8, 1.6, 3.2×10^3 cells/cm^2) and cultured in osteogenic medium. Mineralization was determined by alizarin red staining. Bars (grey and black) differed significantly from their respective controls ($p < 0.01$). (B) Before implantation, cell viability and density was measured by OBS (▲) and BLI (○). Values represent mean $\pm$ SEM ($n = 3$). Trend lines are depicted as dashed lines, for the OBS in black ($r^2 = 0.79$) and for BLI in gray ($r^2 = 0.77$).

interest surrounding the scaffold was defined and within it the scaffold, pore, and bone areas determined. For pore area, the area of proper pores inside and the concave areas on the surface were calculated. To define the latter, a line between the two extremes of the concave surface was drawn. For each image, the total area of pores was related to the bone deposited outside and inside the scaffolds. The total area of new bone was calculated by adding the values of bone inside and outside the pores.

Statistical Analysis

Statistic analysis was performed with Graph Pad Instant Software. Descriptive analyses were performed for all experiments, followed by linear regression analysis, correlation analysis, or one-way ANOVA with a multiple comparison test. All values are expressed as means ± standard error. Significant differences were determined at $p < 0.05$. Power analysis was performed using StatMate2.0 from Graph Pad Software.

RESULTS

Cell Characterization and Preparation of Cell-Based Tissue Engineered Scaffolds

MSC cultures were morphologically heterogeneous and contained polygonal- or fibroblastic-shaped cells with

that retained similar proliferation rates and pluripotency after osteogenic and adipogenic differentiation to the sixth passage (data not shown). Moreover, during osteogenic differentiation, deposition of mineralized matrix was significantly higher ($p < 0.001$) in samples with 1.6×10^3 (O.D. 0.918 ± 0.027) or 3.2×10^3 MSC/cm^2 (O.D. 0.820 ± 0.030) than in those with 0.8×10^3 MSC/cm^2 (O.D. 0.217 ± 0.110) (Fig. 1A).

GFP-positive cells (58%–60%, measured by flow cytometry) produced in vitro a luciferase activity of $1.5–1.8 \times 10^5$ RLU. Cells adhered to the scaffolds in proportion to the seeding concentration as shown by oxygen binding and BLI in vitro proportionate to the seeding density (Fig. 1B, ▲). However, oxygen consumption correlated with bioluminescence intensity only for scaffolds seeded with $>0.125 \times 10^6$ MSCs (Fig. 1B, ○).

In Vivo Monitoring of GFP-Luciferase Transduced MSCs

In the preoperative nondisrupting analysis, oxygen consumption (Fig. 2A) and bioluminescence were proportionate to seeding density only for scaffolds seeded with
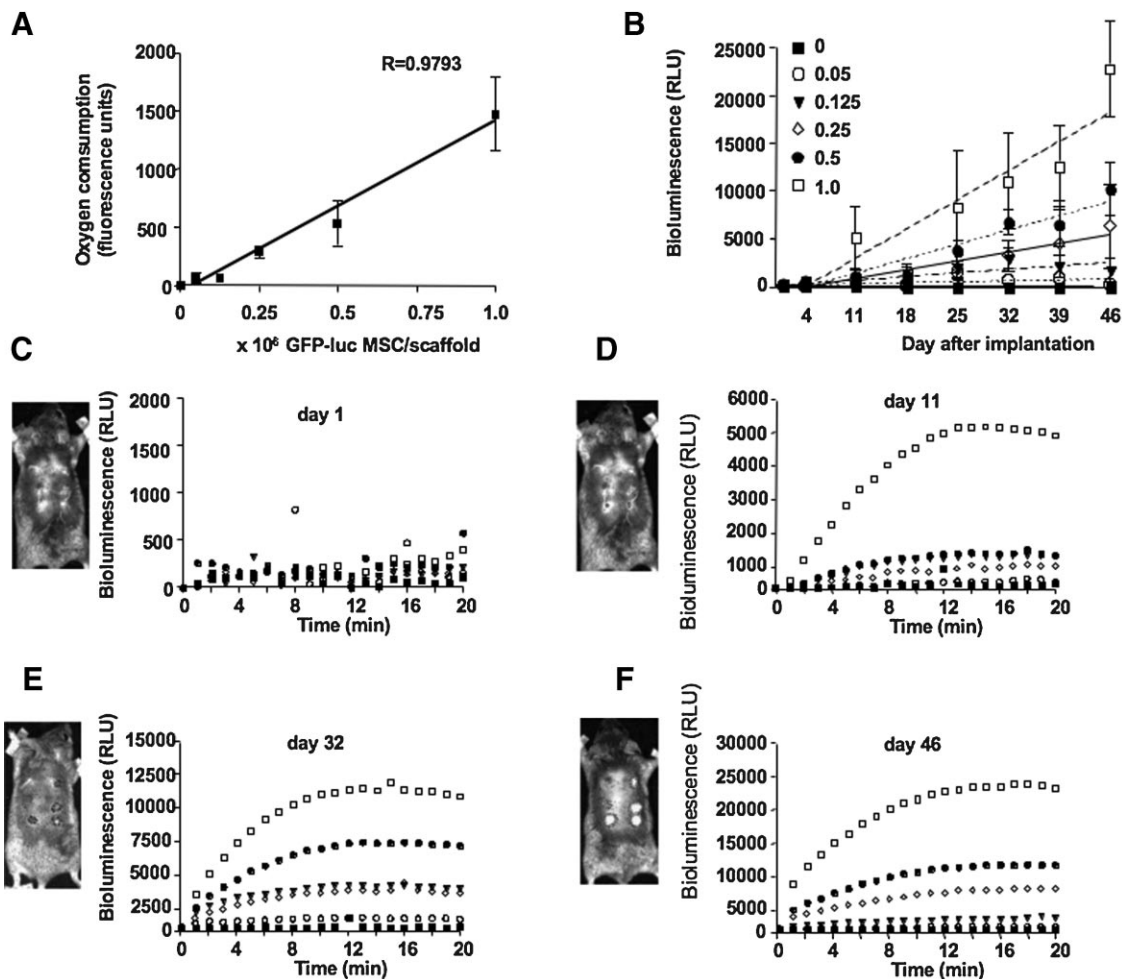

Figure 2. For the first experiment, GFP-luciferase-transduced MSCs were seeded at densities of 0 (■), 0.05 (○), 0.125 (▼), 0.25 (◇), 0.5 (●), or 1 (□) ×10^6 MSCs/scaffold. (A) The OBS assays prior to implantation show linear correlation between the seeding densities and oxygen consumption ($r^2 = 0.98$). (B–F) Kinetics of bioluminescence postoperatively. Values are mean ± SEM ($n = 5$ per group) and lines show measurement trends. (B) The cell number accounts for 26.6% of the total variance ($p = 0.0004$) and the postoperative time accounts for 18.9% of the variance ($p < 0.0001$).

>0.125×10^6 MSCs (data not shown). During the first week after implantation, bioluminescence remained at a low stable level (Fig. 2B, C). At day 11, the signal was 16-fold higher in scaffolds seeded with 1×10^6 MSCs and 6- and 4-fold more intense in those seeded with 0.5 and 0.25×10^6 MSCs, respectively. However, bioluminescence was below the threshold level in scaffolds seeded with 0.125 or 0.05×10^6 MSCs (Fig. 2D). At day 32, the signal was clearly distinguishable from the others. Bioluminescence of the groups followed a distinct kinetic curve, for which the slope and maximum varied relative to the initial number of GFP-luciferase positive MSCs (Fig. 2D–F). Until day 46, bioluminescence further increased in the scaffolds seeded with 1, 0.5, 0.25, and 0.125×10^6 MSCs. In contrast, in scaffolds seeded with 0.05×10^6 MSCs, bioluminescence dropped progressively to a background value, suggesting loss of viable implanted MSCs (Fig. 2E, F).

In the preoperative viability assays, oxygen consumption was 1.6-fold higher in constructs seeded with 1×10^6 MSCs than in those seeded with 0.5×10^6 MSCs (Fig. 3A) instead of the expected 2-fold increase. This suggests that at high seeding concentration, the scaffold surface became saturated. After irradiation, in vitro BLI confirmed that GFP-luciferase transduced MSCs remained viable. A difference in bioluminescence of 1.6-fold was found among the groups seeded at different densities, independent from irradiation (Fig. 3B). In vivo bioluminescence was present in all implants, but the signals did not differ significantly among the groups and remained stable and low until day 11 (Fig. 3C, D). From then on, each group of scaffolds produced a specific bioluminescence profile characterized by a steady increase to a plateau between 14 and 20 min (Fig. 3E). For nonirradiated scaffolds, the bioluminescence intensity reached a higher plateau at higher seeding density (1 or 0.5×10^6 MSCs). This signal increased continuously until day 32 and then remained stable (Fig. 3F, G). In contrast, bioluminescence in every irradiated scaffold persisted at low levels throughout the entire period, suggesting a constant level of viable MSCs (Fig. 3C). A background signal (0–1,000 RLU), was registered for nonseeded scaffolds.

Effect of Cell Irradiation on In Vivo Bone Formation in Tissue Engineered Implants

In scaffolds seeded with 0.5 or 1×10^6 MSCs, new bone occupied 16%–28.6% of the total pore area and constituted considerable surface deposits on the scaffolds (Fig. 4A). Bone formation was 40%–60% lower in scaffolds seeded with 0.5 or 0.25×10^6 MSCs and was as low as 0.7% and 3.3% in irradiated scaffolds (Fig. 4A, C, E). Bone did not form in nonseeded scaffolds (Fig. 4E, right panel). The amount of new bone and the bioluminescence registered at day 46 were proportionate to the initially seeded cell number (Fig. 4B). After preimplantation irradiation of hybrid scaffolds, the correlation in BLI signal and amount of new bone was still present (Fig. 4D).
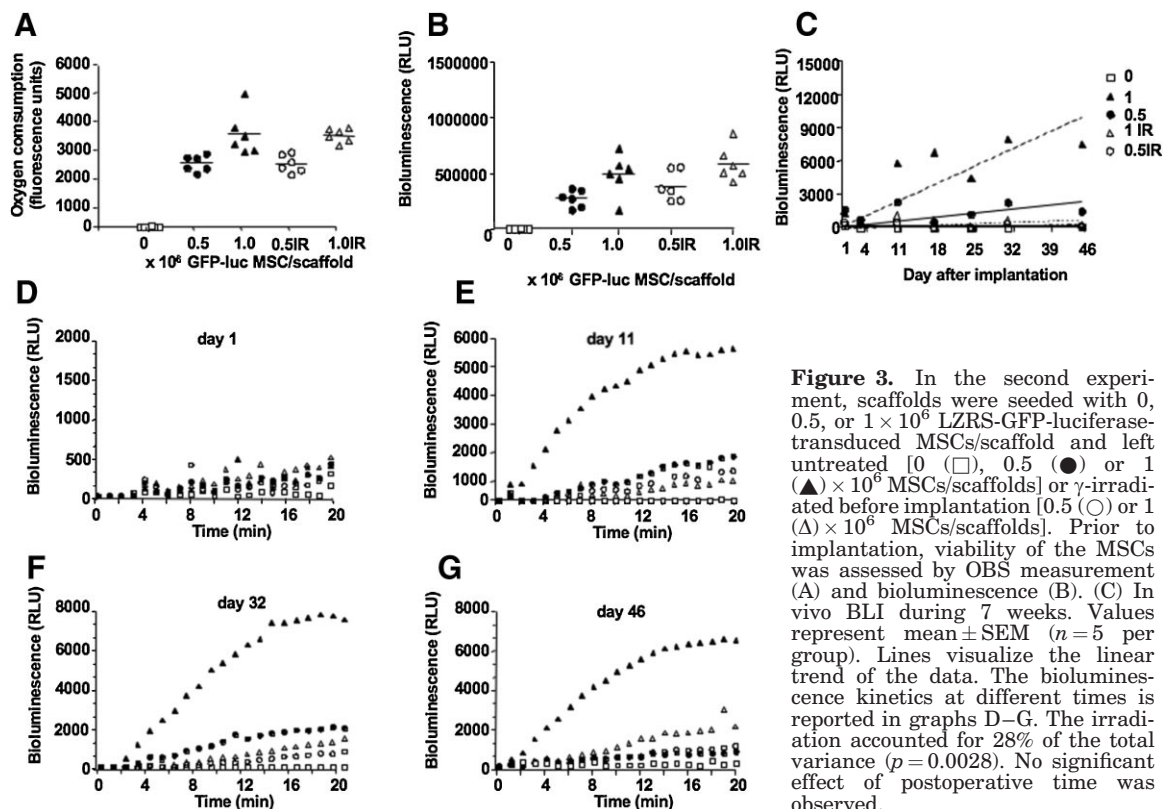

Figure 3. In the second experiment, scaffolds were seeded with 0, 0.5, or 1×10^6 LZRS-GFP-luciferase-transduced MSCs/scaffold and left untreated [0 (□), 0.5 (●) or 1 (▲) $\times 10^6$ MSCs/scaffolds] or γ-irradiated before implantation [0.5 (○) or 1 (Δ) $\times 10^6$ MSCs/scaffolds]. Prior to implantation, viability of the MSCs was assessed by OBS measurement (A) and bioluminescence (B). (C) In vivo BLI during 7 weeks. Values represent mean $\pm$ SEM ($n = 5$ per group). Lines visualize the linear trend of the data. The bioluminescence kinetics at different times is reported in graphs D–G. The irradiation accounted for 28% of the total variance ($p = 0.0028$). No significant effect of postoperative time was observed.
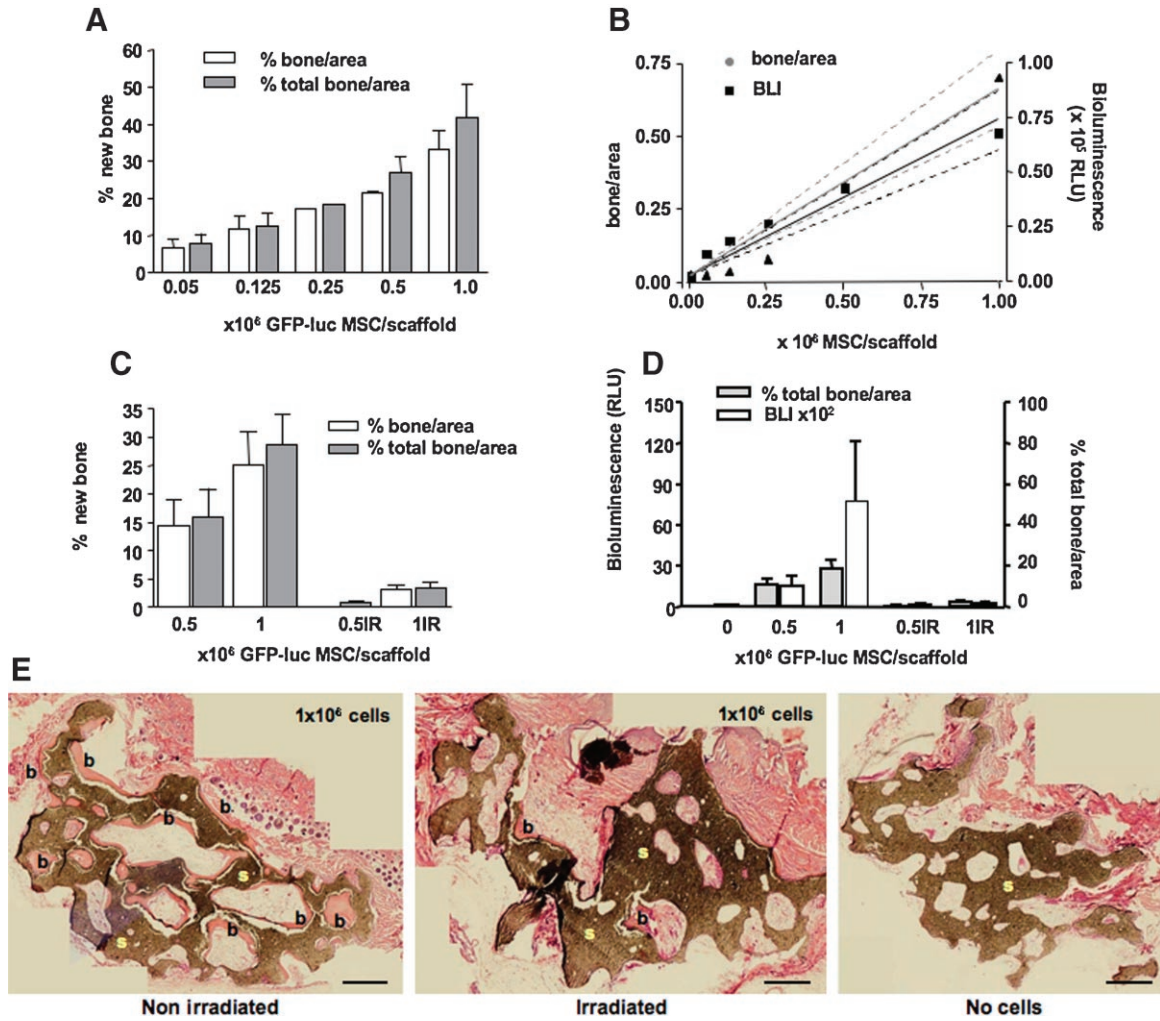
Figure 4. Histomorphometric data of the first (A) and second experiment (C) represent the total bone (gray bars) and the bone deposited inside the pores (white bars). (B, D) The relation between the bioluminescence registered at day 46 and the amount of new bone. Values are means ± SEM. Correlation between cell seeding density and bone deposition ($r^2 = 0.98$) and seeding density and BLI ($r^2 = 0.98$) was observed (B). (D) After irradiation, suppression of BLI signal directly correlated with inhibition of bone formation ($r^2 = 0.87$). (E) Pictures showing bone distribution (b) around and in the scaffolds S is indicated in white (grey areas) in samples seeded with 1×10^6 GFP-luciferase-transduced MSCs/scaffold and nonirradiated (left), irradiated (middle), or nonseeded (right). Scale bars: 0.5 mm. Irradiation of the scaffolds reduced bone formation, with a difference (delta) between the groups of 15.3% (5×10^5 cells seeded) and 24.7% (1×10^6 cells seeded), respectively.

Detection of Osteoclasts and Transplanted MSCs in the Implants

Histology showed GFP-positive MSCs on and in new bone and at the scaffold surface (Figs. Fig. 5A and Fig. 6A, lower panels). No staining was observed in nonseeded implants, and staining was not associated with osteoclasts. New bone showed a woven structure in scaffolds seeded with 0.5×10^6 MSC (experiment 1 and 2) or with 0.25×10^6 MSC (experiment 1). More mature bone (Fig. 5A and Fig. 6A, upper panels) and hematopoietic marrow were seen in implants seeded with 1×10^6 MSCs. In contrast, in scaffolds in which no bone formed, fibrous tissue was found. TRAP staining occurred inside or close to new bone in scaffolds seeded with 1, 0.5, or 0.25×10^6 MSCs (Figs. Fig. 5A and Fig. 6A, middle panels). Osteoclast activity was especially stimulated in scaffolds seeded with the highest densities (Fig. 5B) and in irradiated samples (Fig. 6B).

Finally, small blood vessels perfused all scaffolds to a similar extent, independently of the presence of MSCs or of treatment (Figs. Fig. 5C and Fig. 6C).

DISCUSSION

MSCs are a heterogeneous population of cells of which only a minority are considered to be stem cells with prolonged proliferation potential and pluripotency in vitro. To regenerate bone tissue in vivo, viable MSCs are required, but whether they directly differentiate or retain proliferative capacity is unclear.[17] We applied BLI to an ectopic implantation model to investigate the fate of MSCs in vivo. BLI has proven to be a powerful technology for noninvasive imaging in animal models of oncological diseases and in bone tissue engineering studies[18] and is often used to measure cell proliferation on the basis of luciferase gene expression.[5,6]
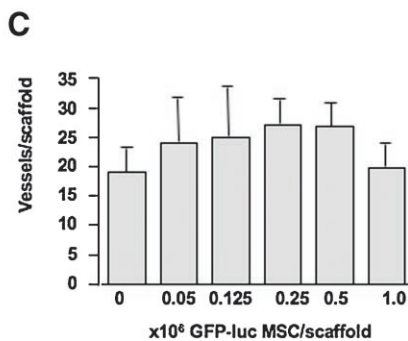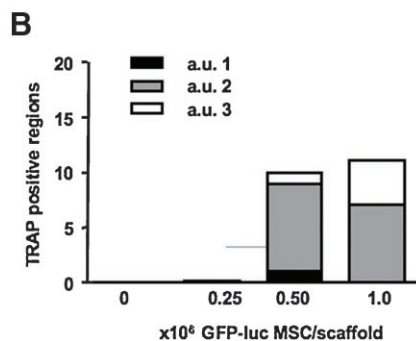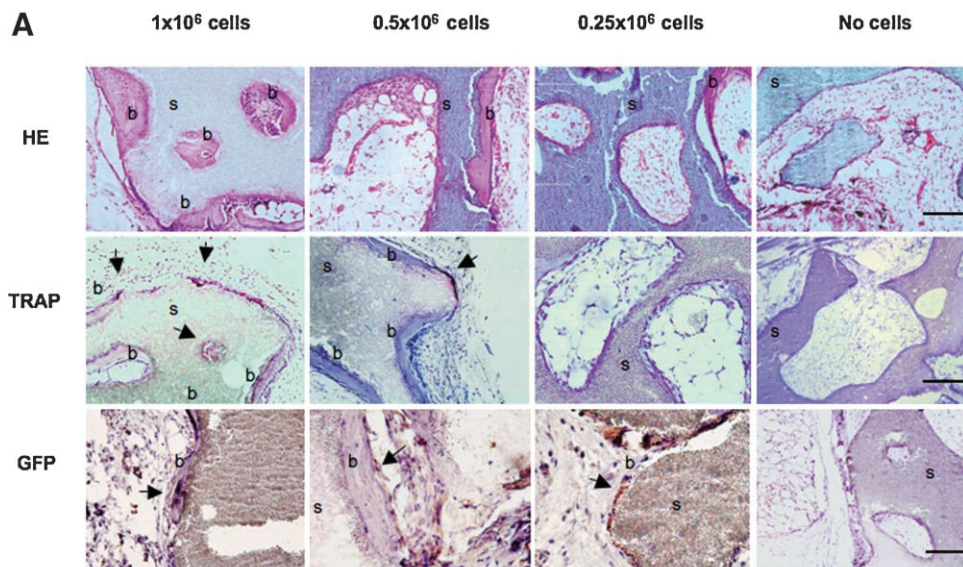
Figure 5. Histology of the first experiment: (A) H&E staining (upper panels), TRAP staining (middle panels; black arrows indicate positive areas; scale bar: 5 μm), and GFP immunolocalization (lower panels; black arrows indicate positive staining; scale bar: 2.5 μm). The bone (b) and scaffolds (s) are indicated. (B) Osteoclast activity was quantified using a score system. (C) Blood vessel quantification from all scaffolds. Scale bars: 0.5 mm.

The luciferase marker gene can be driven by an inducible promoter (specific targeting) or by a constitutively active promoter. In the latter case, a higher BLI intensity is correlated with larger numbers of cells that can only have been produced by cell proliferation.[6,7] Comparable to human or murine MSCs,[19,20] the goat MSCs that we studied display adipogenic and osteogenic differentiation in vitro. In agreement with other reports,[21] cell concentration directly influenced deposition of mineralized matrix and osteogenic differentiation.[22] Mineralization was significantly higher in confluent than in nonconfluent samples. However, at confluence, further increase in cell number did not increase mineralization. We used GFP-luciferase-expressing MSCs to form hybrid scaffolds. We made use of two nondisruptive in vitro assays, oxygen consumption and bioluminescence, to assess seeding efficiency of the implants before surgery. The oxygen consumption assay measures the respiration rate of all living MSCs whereas bioluminescence reflects only the number of luciferase-expressing MSCs, which constitute a little more than half of the total population. Moreover, at high cell density, a 2-fold increase in cell density corresponded to 1.5-fold increase in oxygen consumption, suggesting cell loss due to saturation of the adhesive capacity of the scaffolds.

BLI in vivo showed that cells survived the implantation and remained viable for several weeks, but that a minimal number of cells with proliferation potential had to be present to guarantee increased bioluminescence correlating with bone formation. Then, by irradiation of MSC-seeded scaffolds prior to implantation, we assessed whether the proliferative capacity of the implanted MSCs plays an important role for in vivo bone formation; indeed a small amount of bone was formed in irradiated cell-seeded scaffolds, but far less than in scaffolds that were not irradiated and on which cells retained their proliferative capacity. Apart from the function of seeded MSCs in providing bone-forming cells at an ectopic site, the cells could also secrete matrix or chemokines that might attract host MSCs. This is substantiated by earlier work reporting that established stromal cell cultures remained functional in supporting hematopoiesis after being exposed to extremely high doses of irradiation.[9] Conditioned media obtained from these cultures contained hematopoietic growth factors and cytokines.[11] Others reported that irradiation inhibited proliferation of hMSC up to 2 weeks postirradiation but, thereafter, residual surviving cells regained their normal proliferation rate.[10,12,23]

The fraction of surviving cells depends on irradiation dose[10] but, based on the radiosensitivity of the CFU-F,[12]
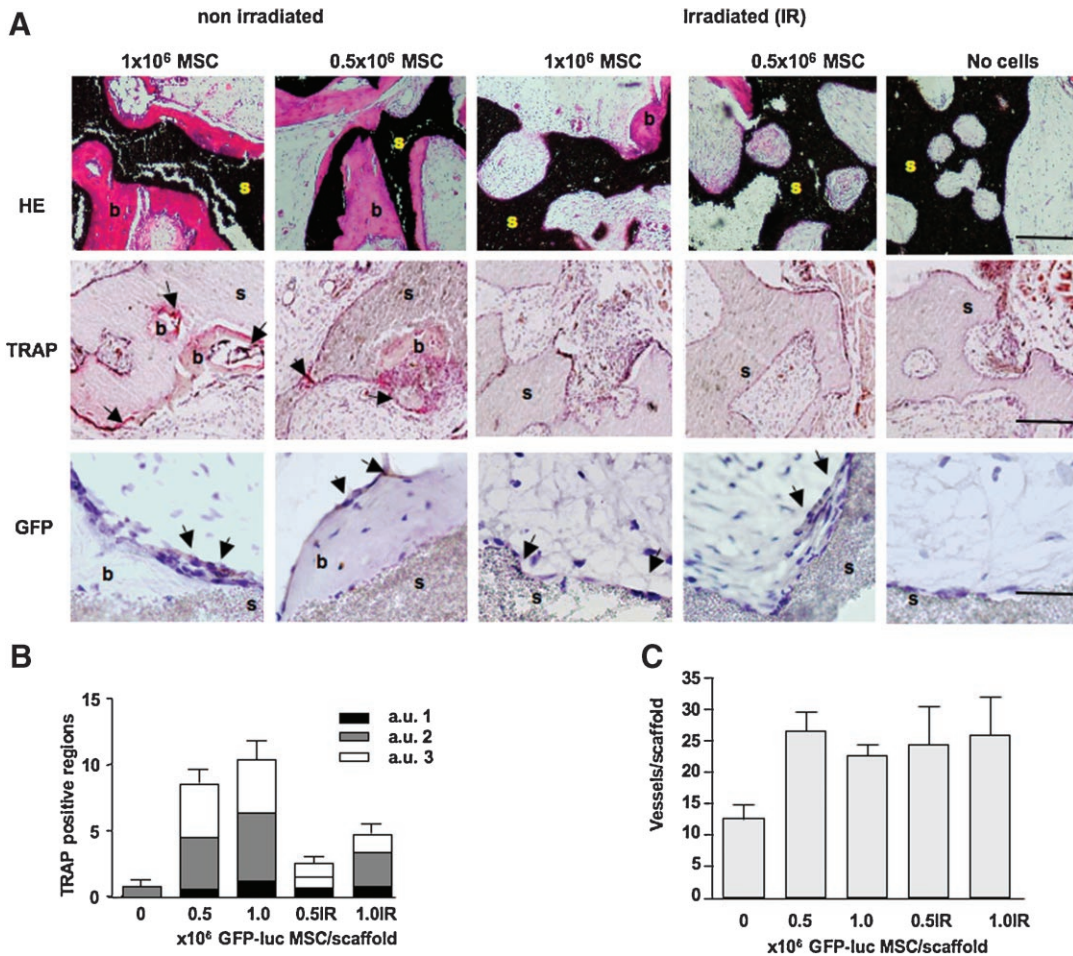
Figure 6. Histology of the second experiment. (A) H&E-staining (upper panels), TRAP staining (middle panels; black arrows indicate positive areas; scale bar: 5 μm), and GFP immunolocalization (lower panels; black arrows indicate positive staining; scale bar: 2.5 μm). Bone (b) and scaffolds (s) are indicated. (B) Osteoclast activity was quantified using a score system. (C) Blood vessels were visible in the pores and outside the scaffold and did not differ significantly in number among the groups. Scale bars: 0.5 mm.

this fraction is on the order of 0.1%–1%. In the irradiated constructs, we abrogated the proliferative capacity of the cells at least temporarily, but not their capacity to secrete matrix or growth factors. We did not measure chemokine or cytokines after implantation, so we cannot exclude that local release of cytokines/chemokines by the seeded MSCs played a role in attracting MSCs from the local environment. However, because minimal bone formation occurred after implantation of irradiated cell-seeded constructs, with much higher bone formation in nonirradiated constructs, we do not consider this likely. We did not use in vivo BrdU incorporation assays to directly show cycling cells in the hybrid scaffolds, mainly because this method cannot discriminate between implanted and resident cells.

GFP-positive cells were found in all cell-seeded constructs, demonstrating the persistence of the implanted MSCs in vivo. This agrees with our earlier experience using low affinity NGFR marker gene to trace seeded goat MSCs.[24] Observation of GFP-positive MSCs within and on the new layer of bone suggests that, besides proliferating in situ, they initiate and participate in neo-osteogenesis by differentiating into osteoblasts and osteocytes. However, we cannot exclude that part of the osteoblasts and osteocytes were of host origin. New bone

was mainly woven. Mineralization and osteoclast activity occurred only in pores wherein a major amount of bone was formed, as indicated by TRAP-positive areas adjacent or within the formed bone. Since the hematopoietic progenitors are negatively selected during in vitro expansion,[25,26] these osteoclasts were probably not derived from implanted MSCs. This suggests a specific remodeling activity, rather than a general inflammatory response to a foreign body. However, a causative relation between bone formation and osteoclast activity remains to be determined. Capillaries and small vessels perfuse each implant, independent of the presence of MSCs, indicating that MSCs were not crucial for angiogenesis.

In vivo proliferation of the MSCs might be required to create a new population of osteoprogenitors, larger than the one derived from direct differentiation of the implanted MSCs. By proliferation, the implanted MSCs would form a conspicuous mass of cells connected to each other via cell–cell interactions, either adherent junctions[27,28] or gap junctions,[29,30] which direct and maintain osteogenic differentiation of the progenitors. In addition, implanted MSCs act as initiators of an osteogenic process subsequently reinforced and overtaken by the host progenitors. During expansion, MSCs might provide a

local gradient of chemokines that attracts circulating host progenitors and stimulates the onset of osteo-specific genes[31,32] and the secretion of mineralized matrix and growth factors. The recruitment of host cells might occur via the capillaries.[32,33] In view of TRAP activity in our constructs, it is tempting to speculate that the host system might recognize the construct as an osteogenic particle capable of recruiting osteoclasts to form a so-called bone multicellular unit in which bone deposition and bone readsorption are spatially coupled in the remodeling process necessary to the further bone deposition.[34–37]

In conclusion, we demonstrated that bone deposition in in vivo tissue engineered constructs depends on a minimal number of stem cells and that interference with their proliferative capacity by irradiation severely reduces bone formation. We suggest that bioluminescence may be used as an indicator of proliferation or death of seeded MSCs in the implants.

ACKNOWLEDGMENTS

REFERENCES

1. Wan C, He Q, McCaigue M, et al. 2006. Nonadherent cell population of human marrow culture is a complementary source of mesenchymal stem cells (MSCs). J Orthop Res 24: 21–28.
2. Kon E, Muraglia A, Corsi A, et al. 2000. Autologous bone marrow stromal cells loaded onto porous hydroxyapatite ceramic accelerate bone repair in critical-size defects of sheep long bones. J Biomed Mater Res 49:328–337.
3. Kruyt MC, de Bruijn JD, Yuan H, et al. 2004. Optimization of bone tissue engineering in goats: a preoperative seeding method using cryopreserved cells and localized bone formation in calcium phosphate scaffolds. Transplantation 77:359–365.
4. Petite H, Viateau V, Bensaid W, et al. 2000. Tissue-engineered bone regeneration. Nat Biotechnol 18:959–963.
5. Bar I, Zilberman Y, Zeira E, et al. 2003. Molecular imaging of the skeleton: quantitative real-time bioluminescence monitoring gene expression in bone repair and development. J Bone Miner Res 18:570–578.
6. Blum JS, Temenoff JS, Park H, et al. 2004. Development and characterization of enhanced green fluorescent protein and luciferase expressing cell line for non-destructive evaluation of tissue engineering constructs. Biomaterials 25:5809–5819.
7. Leo BM, Li X, Balian G, et al. 2004. In vivo bioluminescent imaging of virus-mediated gene transfer and transduced cell transplantation in the intervertebral disc. Spine 29: 838–844.
8. Pelled G, Tai K, Sheyn D, et al. 2007. Structural and nanoindentation studies of stem cell-based tissue-engineered bone. J Biomech 40:399–411.
9. Zuckerman KS, Prince CW, Rhodes RK, et al. 1986. Resistance of the stromal cell in murine long-term bone marrow cultures to damage by ionizing radiation. Exp Hematol 14:1056–1062.
10. Li J, Kwong DL, Chan GC. 2007. The effects of various irradiation doses on the growth and differentiation of marrow-derived human mesenchymal stromal cells. Pediatr Transplant 11:379–387.
11. Gualtieri RJ. 1987. Consequences of extremely high doses of irradiation on bone marrow stromal cells and the release of hematopoietic growth factors. Exp Hematol 15:952–957.
12. Bierkens JG, Hendry JH, Testa NG. 1989. The radiation response and recovery of bone marrow stroma with particular reference to long-term bone marrow cultures. Eur J Haematol 43:95–107.
13. Day RN, Kawecki M, Berry D. 1998. Dual-function reporter protein for analysis of gene expression in living cells. Biotechniques 25:848–854,856.
14. Yuan H, Van Den Doel M, Li S, et al. 2002. A comparison of the osteoinductive potential of two calcium phosphate ceramics implanted intramuscularly in goats. J Mater Sci Mater Med 13:1271–1275.
15. Weijer K, Uittenbogaart CH, Voordouw A, et al. 2002. Intrathymic and extrathymic development of human plasmacytoid dendritic cell precursors in vivo. Blood 99:2752–2759.
16. Erlebacher A, Derynck R. 1996. Increased expression of TGF-beta 2 in osteoblasts results in an osteoporosis-like phenotype. J Cell Biol 132:195–210.
17. Kruyt MC, de Bruijn JD, Wilson CE, et al. 2003. Viable osteogenic cells are obligatory for tissue-engineered ectopic bone formation in goats. Tissue Eng 9:327–336.
18. de Boer J, van Blitterswijk C, Löwik C. 2006. Bioluminescent imaging: emerging technology for non-invasive imaging of bone tissue engineering. Biomaterials 27:1851–1858.
19. Grafi G, Avivi Y. 2004. Stem cells: a lesson from dedifferentiation. Trends Biotechnol 22:388–389.
20. Ratajczak MZ, Kucia M, Majka M, et al. 2004. Heterogeneous populations of bone marrow stem cells—are we spotting on the same cells from the different angles? Folia Histochem Cytobiol 42:139–146.
21. Purpura KA, Aubin JE, Zandstra PW. 2004. Sustained in vitro expansion of bone progenitors is cell density dependent. Stem Cells 22:39–50.
22. Chambers TJ. 2000. Regulation of the differentiation and function of osteoclasts. J Pathol 192:4–13.
23. Friedenstein AJ, Latzinik NV, Gorskaya UF, et al. 1981. Radiosensitivity and postirradiation changes of bone marrow clonogenic stromal mechanocytes. Int J Radiat Biol Relat Stud Phys Chem Med 39:537–546.
24. Kruyt MC, Stijns MM, Fedorovich NE, et al. 2004. Genetic marking with the DeltaLNGFR-gene for tracing goat cells in bone tissue engineering. J Orthop Res 22:697–702.
25. Quinn JM, Whitty GA, Byrne RJ, et al. 2002. The generation of highly enriched osteoclast-lineage cell populations. Bone 30:164–170.
26. Udagawa N, Takahashi N, Yasuda H, et al. 2000. Osteoprotegerin produced by osteoblasts is an important regulator in osteoclast development and function. Endocrinology 141:3478–3484.
27. Castro CH, Shin CS, Stains JP, et al. 2004. Targeted expression of a dominant-negative N-cadherin in vivo delays peak bone mass and increases adipogenesis. J Cell Sci 117:2853–2864.
28. Ferrari SL, Traianedes K, Thorne M, et al. 2000. A role for N-cadherin in the development of the differentiated osteoblastic phenotype. J Bone Miner Res 15:198–208.
29. Gramsch B, Gabriel HD, Wiemann M, et al. 2001. Enhancement of connexin 43 expression increases proliferation and differentiation of an osteoblast-like cell line. Exp Cell Res 264:397–407.
30. Stains JP, Lecanda F, Screen J, et al. 2003. Gap junctional communication modulates gene transcription by altering the recruitment of Sp1 and Sp3 to connexin-response elements in osteoblast promoters. J Biol Chem 278:24377–24387.
31. Bellows CG, Heersche JN, Aubin JE. 1990. Determination of the capacity for proliferation and differentiation of osteopro-

genitor cells in the presence and absence of dexamethasone. Dev Biol 140:132–138.

32. Kale S, Biermann S, Edwards C, et al. 2000. Three-dimensional cellular development is essential for ex vivo formation of human bone. Nat Biotechnol 18:954–958.

33. Parfitt AM. 1998. Osteoclast precursors as leukocytes: importance of the area code. Bone 23:491–494.

34. Parfitt AM. 2002. Targeted and nontargeted bone remodeling: relationship to basic multicellular unit origination and progression. Bone 30:5–7.

35. Hauge EM, Qvesel D, Eriksen EF, et al. 2001. Cancellous bone remodeling occurs in specialized compartments lined by cells expressing osteoblastic markers. J Bone Miner Res 16:1575–1582.

36. Martin TJ, Sims NA. 2005. Osteoclast-derived activity in the coupling of bone formation to resorption. Trends Mol Med 11:76–81.

37. Moroz A, Crane MC, Smith G, et al. 2006. Phenomenological model of bone remodeling cycle containing osteocyte regulation loop. Biosystems 84:183–190.